

## The High Frequency Instrument of Planck: Design and Performances

J.M. Lamarre<sup>1</sup>, P.A.R. Ade<sup>2</sup>, A. Benoît<sup>3</sup>, P. de Bernardis<sup>4</sup>, J. Bock<sup>6</sup>, F. Bouchet<sup>5</sup>, T. Bradshaw<sup>7</sup>, J. Charra<sup>1</sup>, S. Church<sup>8</sup>, F. Couchot<sup>9</sup>, J. Delabrouille<sup>1,10</sup>, G. Efstathiou<sup>11</sup>, M. Giard<sup>12</sup>, Y. Giraud-Héraud<sup>13</sup>, R. Gispert<sup>1</sup>, M. Griffin<sup>2</sup>, A. Lange<sup>8</sup>, A. Murphy<sup>14</sup>, F. Pajot<sup>1</sup>, J.L. Puget<sup>1</sup>, I. Ristorcelli<sup>12</sup>

1 *Institut d'Astrophysique Spatiale, Univ. Paris XI, F-91405 Orsay Cedex, France*

2 *Queen Mary and Westfield College, Physics Department, Mile End Road, E1 4NS London, U.K.*

3 *Centre de Recherche des Très Basses Températures, 25 avenue des Martyrs, BP 166, F-38042 Grenoble cedex 9, France*

4 *Univ. La Sapienza, Dipartimento di Fisica G. Marconi, Grupo di Cosmologia Sperimentale, Piazzale A. Moro, I-00185 Roma, Italy*

5 *Institut d'Astrophysique de Paris, 98bis Bd Arago, F-75014 Paris, France*

6 *Jet Propulsion Laboratory, Mail 424-49 - Caltech, CA 91125 Pasadena, USA*

7 *Rutherford Appleton Laboratory, Chilton, Didcot, OX 11 0QX Oxfordshire, U.K.*

8 *California Institute of Technology, Observational Cosmology - Mailstop 59-33, 1201 E. California, CA91125 Pasadena, USA*

9 *IN2P3, LAL, bat.200, Université Paris XI, F-91405 Orsay Cedex, France*

10 *Enrico Fermi Institute, Univ. of Chicago, 5460 S. Ellis Ave., Chicago, IL 60637, USA*

11 *Institute of Astronomy, Madingley road, CB3 0HA Cambridge, United Kingdom*

12 *Centre d'Etude Spatiale des Rayonnements, 9 Av. du Colonel Roche, BP 4346, F-31029 Toulouse Cedex, France*

13 *PCC, Collège de France, 11 Place M. Berthelot, F-75231 Paris Cedex 05, France*

14 *Experimental Physics, Nat. Univ. of Ireland, Co. Kildare - Maynooth, Ireland*

### 1. INTRODUCTION

The PLANCK High Frequency Instrument (HFI) will utilise 100 mK bolometers to measure the anisotropies of the Cosmic Microwave Background (CMB) at all scales larger than 5 arcminutes to an unprecedented accuracy of  $\Delta T/T = 2 \times 10^{-6}$  per resolution element. These measurements will be limited mainly by the fundamental limits set by photon noise from the CMB and the thermal emission of the telescope (Lamarre et al., 1995) and astrophysical foregrounds. Furthermore the very high sensitivity of the PLANCK HFI will allow precise measurements of the polarization of the CMB.

The PLANCK CMB measurements will enable cosmologists to test models for the origin and structure of the Universe (quantum fluctuations or topological defects) and to constrain the key 10–20 cosmological parameters defining our Universe to an accuracy of the order of a percent or better in most scenarios. Since Hubble's discovery of the expansion of the Universe, much effort has been devoted to establishing the geometrical and kinematic characteristics of our universe (Hubble constant, deceleration parameter, cosmological constant, curvature,....). The precise constraints

on these and other parameters from PLANCK (and particularly PLANCK HFI) will far surpass the accuracy of conventional astronomical techniques, heralding a new era in Cosmology.

In the next section of this paper, we shortly describe the rationale that allowed to define the main properties of the HFI. The third section is dedicated to the description of the instrument and its expected performances.

## 2. ASTROPHYSICAL CONFUSION AND SYSTEMATIC EFFECTS

At the level of sensitivities required to recover interesting information from CMB anisotropies, it is expected that astrophysical foregrounds may induce unwanted fluctuations of the sky brightness in the frequency range of interest. The main contributors to these foregrounds arise from the emission of our Galaxy and are strongly concentrated towards the galactic plane. Three main processes contribute to the galactic emission in the interesting frequency band between 10 and 1000 GHz: greybody emission from interstellar dust, synchrotron emission from electrons moving in the galactic magnetic field, and bremsstrahlung (or free-free) emission of electrons off nuclei.

On most of the sky (away from the galactic plane), at frequencies around 100 GHz, the amplitude of CMB fluctuations is expected to be, on average, an order of magnitude higher than that of fluctuations due to other processes. Nonetheless, the exact contribution of foregrounds should be known in order to quantify the contribution from primary CMB fluctuations (and thus get an accurate and reliable determination of cosmological parameters). Furthermore, each of the individual processes described above is by itself interesting for astrophysics or cosmology (in particular for the physics of galaxies, of clusters of galaxies, and for structure formation).

In order to allow disentangling the various components of the sky emission, the HFI will map the Far Infrared sky in six channels covering the frequency range from 90 GHz to 960 GHz. This wide frequency coverage has been chosen so that the HFI can measure the two main foregrounds at these frequencies, Galactic dust emission and distant infrared galaxies. For these, the spectra are steeply rising with frequency allowing a measurement of these foregrounds with an angular resolution as good as the one achieved on the CMB measurements or better. These foregrounds are now much better understood as a result of all sky surveys constructed with the DIRBE and FIRAS instruments aboard COBE, recent ISO observations and ground based follow-up observations.

The HFI frequencies have been carefully chosen to optimize also the detection of clusters of galaxies via the Sunyaev-Zeldovich (S-Z) effect. This effect arises from the Compton interaction of CMB photons with the hot gaseous atmospheres of clusters of galaxies. The S-Z effect is expected to be the dominant secondary distortion of the CMB, but can be separated very accurately from the primordial CMB anisotropies via its unique spectral signature. The HFI should detect thousands of S-Z clusters of galaxies, probing redshifts  $z \sim 1$ . The HFI will also detect thousands of infrared

galaxies. The production of complete near all-sky catalogues of galaxy clusters and infrared galaxies with the HFI are important scientific goals of the PLANCK mission.

Detailed models of the millimeter and submillimeter sky, including polarization, have been undertaken to analyse the performance of the HFI. With the HFI design proposed here, we have demonstrated that the primordial CMB anisotropies can be recovered with an accuracy that is limited only by the precision with which we can subtract foregrounds (Bouchet et al., 1996, Gispert and Bouchet, 1996). The most sensitive channel for both the intensity and the polarization anisotropies is at 217 GHz and has an angular resolution of 5.5 arcminutes. The full frequency range of the HFI instrument provides, in addition to excellent monitoring and subtraction of foregrounds and the S-Z effect, some redundancy against partial instrument failures. With our present understanding of foregrounds, the accuracy of the primordial CMB reconstruction is improved by combining HFI and LFI data. The addition of LFI data enables more accurate removal of the low frequency foregrounds (free-free and synchrotron emission). The full PLANCK payload (HFI and LFI) provides essential cross-checks of systematic errors (e.g. thermal variations,  $1/f$  noise and stray-light) and of any unexpected behaviour of the foregrounds. The cosmological results from PLANCK will thus be as free as possible from systematic errors and any a priori hypotheses concerning foregrounds.

The PLANCK sky scanning strategy can be chosen to optimize the redundancy in the data by moving the spin axis by up to 10 deg from the antisolar direction. An optimized scanning strategy is essential for detecting, controlling and removing systematic effects which might affect the data (Delabrouille et al., this conference). A full pipeline including modules to test and remove all identified systematic effects will be ready and fully tested one year before launch.

### 3. THE PLANCK HIGH FREQUENCY INSTRUMENT

#### 3.1 Architecture

The HFI consists of (i) the HFI focal plane unit, (ii) the readout electronics, (iii) the Data Processing Unit, (iv) the coolers, and (v) harness and tubes linking various subsystems.

The scientific objectives require both a high sensitivity and a time response fast enough to scan 5 arcmin beams at 6 degrees per second. With the best available technology this can be achieved only with bolometers cooled at about 100 mK or less, which is a major requirement that drives the architecture of the HFI. This is achieved, starting from the passively cooled 50K/60K stage of the payload module, by a four-stage cooling system (18K-4K-1.6K-0.1K) detailed in section 3.6. The 18K cooler is common to the HFI and the Low Frequency Instrument (LFI). The 4K stage protects the inner stages from the thermal radiation of the 18K environment. It provides also an electromagnetic shielding (a Faraday cage) for the high impedance part of the readout electronics. It is the envelope of the HFI focal plane unit.

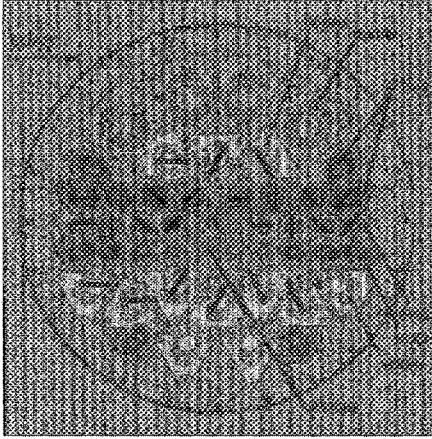


FIGURE 1. View of the entrance horns as seen from the telescope. Lines across horns represent the direction of the measured polarization, when applicable. (See Color Plate II).

The focal plane of the *PLANCK* HFI is a layout of 48 pixels fulfilling all the requirements set by scientific objectives of astrophysical component separation optimisation as well as other data reduction constraints. It is necessary that the HFI has enough pixels at each frequency in the cross scan direction to ensure proper sampling of the sky as the satellite spin axis is depointed in steps of 3 to 5 arc minutes, and fulfills the requirement that detectors at the same frequency but different polarisation angles must follow each other on the same scanning path to allow direct differences to be made. Polarized bolometers are grouped by three or four depending on the channel, and their relative orientations are optimized for the measurement of Stokes parameters (Couchot *et al.*, 1998). Having several detectors (and at least two sets of complementary polarised detectors) for each channel also provide improved sensitivity, improved immunity to cosmic rays and redundancy.

The coupling of the telescope with the detectors is made by corrugated horns attached on the 4K stage, the aperture of the waveguides being the only radiative coupling between the inside and the outside of the 4K box. The HFI focal plane unit has an extension to the 18K and 50/60K stages, enclosing the first stage of the preamplifiers (J-FETs at 120K).

### 3.2 Sensitivity

Table 1 gives the mean sensitivity per pixel for a mission duration of 14 months. Total bolometer noise is assumed to be equal to 1.4 times photon noise. Pixels are assumed to be square (side = beam Full Width at Half Maximum).  $\Delta T/T$

| Central frequency ( $\nu$ )          | GHz       | 100  | 143  | 217  | 353  | 545 | 857  |
|--------------------------------------|-----------|------|------|------|------|-----|------|
| Beam Full Width Half Max.            | arcmin    | 10.7 | 8.0  | 5.5  | 5.0  | 5.0 | 5.0  |
| Number of unpolarised det.           |           | 4    | 3    | 4    | 6    | 0   | 6    |
| $\delta T/T$ Sensitivity (Intensity) | $\mu K/K$ | 1.7  | 2.0  | 4.3  | 14.4 | 147 | 6670 |
| Number of polarised det.             |           | 0    | 9    | 8    | 0    | 8   | 0    |
| $\delta T/T$ Sensitivity (U and Q)   | $\mu K/K$ |      | 3.7  | 8.9  |      | 208 |      |
| Flux Sensitivity per pixel           | mJy       | 8.7  | 11.5 | 11.5 | 19.4 | 38  | 43   |
| $y_{SZ}$ per FOV ( $\times 10^6$ )   |           | 1.11 | 1.88 | 547  | 6.44 | 26  | 600  |

Table 1: HFI sensitivities.

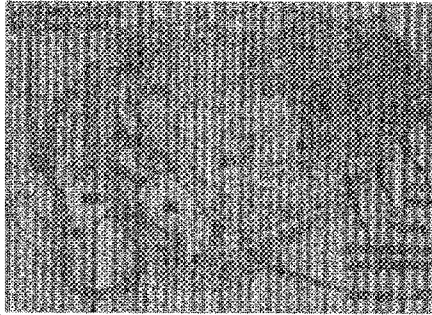


FIGURE 2. Architecture of the HFI focal plane unit. (See Color Plate III).

sensitivity is the noise expressed in CMB temperature relative change ( $1\sigma$ ).  $y_{SZ}$  is the sensitivity ( $1\sigma$ ) to the comptonisation factor for the Sunyaev-Zeldovich effect.

### 3.3 Optics

To detect anisotropies at a level of 1 part in  $10^6$  in the CMB it is essential that the sensitivity of the HFI to unwanted energy is minimised, both from the point of view of beam directivity and spectral purity. This is obtained thanks to an original architecture tightly coupling optical and cryogenic designs (Figure 2).

In the angular domain, i.e. for scattered and diffracted waves, a high rejection ratio must be achieved between the main beam and the side lobes. For that purpose, the field of view of the HFI detectors is determined by naked corrugated horns in the focal plane which have a well determined angular response thereby allowing control of the stray fields whilst coupling efficiently to the energy from the main beam.

By using back-to-back horns at 4K (Figure 3) a beam waist is produced at the 1.6K level where spectral filters are placed to define the detected band. A third

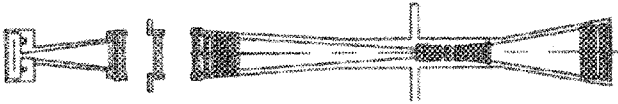


FIGURE 3. Schematic of optical layout for a single HFI pixel with, at 0.1K (left), the bolometer, its horn, and its filters, at 1.6K (centre) filters, and at 4K (right) filters and back-to-back horns.

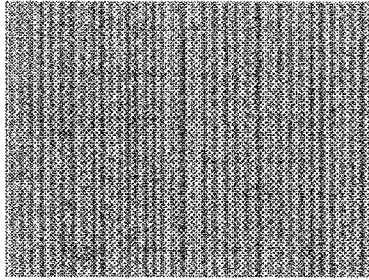


FIGURE 4. Far field beam pattern for HFI 143GHz feed.

horn re-images radiation onto the bolometric detector. This design naturally offers thermal breaks between the 100mK detectors, the warmer 1.6K filters and the focal plane horns at 4K. This scheme also allows some flexibility to choose where the unwanted thermal power is dumped (i.e. 4K, 1.6K or 100mK) and allows to reach the very small radiative heat loads (a few nW) required on the 100mK stage. The far field pattern obtained with the design of figure 3 is shown in figure 4.

Since most sources of spurious radiation have a steep spectrum, a high spectral rejection is mandatory. In addition, the radiation of the filters themselves on the detectors, and the load from warm parts on the cryogenic stages must be kept small. The needed rejection of the broadband emission from the sky and telescope requires a sequence of filters to guarantee the spectral purity of the final measurements. Currently the spectral bands are defined by a combination of the high pass waveguide cut-on between the front back-to-back horns and a low pass metal mesh filter cut-off. Because of the requirements to minimise harmonic leaks we add four additional low pass edge filters such that the overall rejection exceeds  $10^{10}$  at higher frequencies. This scheme also allows some flexibility to choose where the unwanted thermal power is dumped (i.e. 4K, 1.6K or 100mK). The measured spectral performance for a prototype 143GHz band filter set is given in Figure 5. The characteristic is shown for each filter along with the overall system transmission. As can be seen, the overall filter transmission is about 55% while the rejection increases from  $10^{10}$  to  $10^{12}$  not accounting for the cut-off of the final filter. These characteristics fulfil the spectral purity requirement for HFI channels.

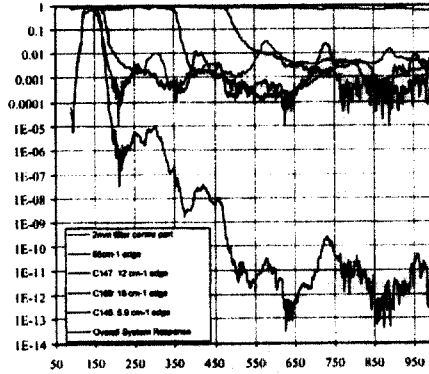


FIGURE 5. Plot of Prototype 143GHz Channel Spectral Response (horizontal axis in GHz). (See Color Plate IV).

| Channel                     | 100  | 143  | 143p | 217  | 217p | 353  | 545p | 857  |
|-----------------------------|------|------|------|------|------|------|------|------|
| $\tau$ (ms)                 | 4.6  | 3.2  |      | 2.1  |      | 2.0  | 2.0  | 2.0  |
| $NEP_{bol} \times 10^{17}$  | 0.82 | 0.90 |      | 1.04 |      | 1.16 | 1.51 | 3.80 |
| $NEP_{phot} \times 10^{17}$ | 1.01 | 1.24 | 0.88 | 1.49 | 1.05 | 2.88 | 4.66 | 14.6 |

Table 2: Requirements on detectors, assuming a 1rpm scan rate and we take 2 time constants ( $2\tau$ ) per beam. Noise Equivalent Power is in  $W/\sqrt{Hz}$

### 3.4 Bolometric detectors

The HFI sensitivity requirements have been determined from the fundamental constraints of photon noise originating from the 3K CMB radiation itself at the longer wavelengths and the residual emission from the telescope and instrument at the shorter wavelengths. Specifically then, the PLANCK HFI bolometric detectors require inherent NEPs of less than or equal to the quadratic sum of the noises from the background components together with a speed of response fast enough to preserve all of the signal information at the 1 rpm scan rate of the satellite. The current baseline detectors, which provide the required sensitivity and response speed are CalTech/JPL spider bolometers. These requirements are summarised in Table 2. A prototype bolometer, CSK18, has been built with time constant and NEP close to those needed for the 100 GHz channel.

### 3.5 Electronics

The HFI electronics consists mainly of a Digital Processor Unit (DPU), the drive

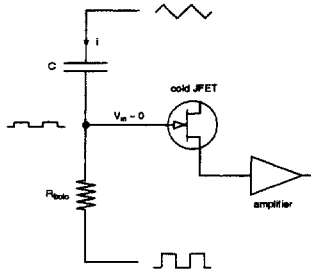


FIGURE 6. Principle of bolometer readout.

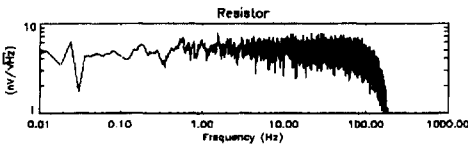


FIGURE 7. Noise power spectrum of readout electronics on a  $3k\Omega$  test resistor at ambient temperature (same Johnson noise as a  $10M\Omega$  resistor at 100mK).

electronics of the three coolers (20K, 4K, and 0.1K) and the readout electronics of the bolometers and high precision thermometers.

The readout electronics has been specially developed for the HFI. It is able to give a readout over the frequency range needed for PLANCK, i.e. 0.016Hz to about 100Hz (Gaertner *et al.*, 1997). This system uses a differential AC bias current and has a uniform noise performance:  $\leq 5nV/\sqrt{Hz}$ . Its principle is shown on figure 6. The capacitive load at 100K does not introduce additional Johnson noise, as would a resistor.

This system allows a full control of the current and voltage of the measured bolometer, so that in flight optimisation of the bolometer impedance will be possible:  $V(I)$  measurements and  $(S/N)(I)$  on the CMB dipole and the galaxy. Two dedicated heaters will allow to perform the temperature control of the 0.1K stage. A total number of 66 measurement chains reads 48 bolometers, 16 thermometers, and 2 test devices.

### 3.6 Cryogenics

The sensitivity of the HFI critically depends on the temperature of the detectors. The cooling scheme that allows to cool at 0.1K the 48 bolometers and their filters is based on technical solutions that have been successfully tested in flight or have been demonstrated on ground applications and are being qualified for space. Each



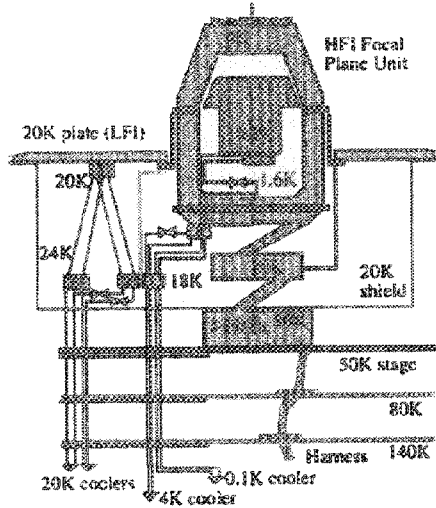


FIGURE 8. Scheme of the cooling system

cooling system takes advantage of the previous one in an optimal way, following the arrangement of Figure 8.

The precooling of the instrument to 50/60K is insured by the PLANCK Payload Module thanks to passive radiation to free space, which can be very efficient in the environment of the Earth-Sun Lagrangian L2 orbit of PLANCK.

A closed cycle cooler using Joule-Thomson (J-T) expansion of hydrogen and sorption compressors insure cooling of both the LFI and the HFI at about 20K (Wade, 1991). The J-T valve delivers a mixture of liquid and gas at about 17.5K. A first high efficiency heat exchanger cools at 18K the helium flows of the 4K and the 0.1K stages. This heat exchanger is thermally decoupled from the one used to cool the LFI 20K plate, for which a larger temperature drop in the exchanger is acceptable. The shielded cable from the 4K box to the JFET box is thermally attached to the 20K stage in order to reduce heat loads on the 4K stage. Joule-Thomson expansion of helium compressed by mechanical compressors is used to cool the 4K stage of the HFI (Bradshaw et al., 1997). That stage supports the back-to-back horns that insure the optical coupling of the detectors with the telescope.

Lower temperature are obtained at 0.1K by dilution of  $^3\text{He}$  in  $^4\text{He}$  (Benoit, 1997). A 1.6K stage is generated by J-T expansion of mixed helium. This stage supports filters and intercepts heat from the 4K stage. The 0.1K stage supports the bolometers, thermometers, heaters, and filters. Its temperature is controlled thanks to a closed loop active system. The additional cooling power available from

the mixture of  $^3\text{He}$  and  $^4\text{He}$  under 1.6K is used to intercept heat inputs along the mechanical support of the 0.1K stage.

The tubes from and to each stage are attached to form heat exchangers for all circulating fluids in order to minimise thermal losses.

### 3.7 Calibration

The HFI PLANCK experiment has no on-board calibrator. The in-orbit calibration will provide the accuracy (about 1%) needed for the data processing. It will use the measurement of the galactic emission by the FIRAS experiment and on that of the CMB dipole by the DMR experiment to calibrate respectively the higher and the lower frequency channels. The final photometric calibration will be adjusted on the FIRAS calibration after proper averaging of large enough regions on the sky. The pattern of the main beam will be measured using the outer planets. The far side-lobes will be recovered using the galactic emission, the sun, and the earth.

A calibration facility will allow to measure prior to launch the HFI spectral response with the needed accuracy, and to get a first measurement of the other main parameters of the instrument, which will be the most complete test of the instrument before launch.

## 4. ACKNOWLEDGEMENTS

The design of the HFI was possible due to contributions of number of engineers in the participating institutes and thanks to the funding provided by national agencies in France, United Kingdom, USA, Ireland, and Italy. It also benefited from the cooperative work of the HFI team with ESTEC and industry during the feasibility phase.

## REFERENCES

- A. Benoit, Proc. of the ESA Symposium ESA SP-400 (1997)
- F. R. Bouchet, R. Gispert, F. Boulanger & J.-L. Puget, Proceedings of the XVth Moriond Astrophysics meeting, 1996, edited by F.R. Bouchet, R. Gispert, B. Guiderdoni and J. Tran Thanh Van, éditions Frontières, 481
- T.W. Bradshaw and A.H. Orlowska, Proc. of the ESA Symposium ESA SP-400 (1997)
- F. Couchot, J. Delabrouille, J. Kaplan & B. Revenu Accepted for publication in A&A, (astro-ph/9807080)
- S. Gaertner et al., Astron. Astrophys. Suppl. Ser. 126, 151-160 (1997)
- R. Gispert, & F. R. Bouchet, Proceedings of the XVth Moriond Astrophysics meeting, 1996, edited by F.R. Bouchet, R. Gispert, B. Guiderdoni and J. Tran Thanh Van, éditions Frontières, 503
- J.-M. Lamarre, F.-X. Desert, T. Kirchner, Space Science Reviews, 74, 1995, pp27-36.
- L. Wade, Adv. in Cryogenic Eng., Plenum Press, New York, 37 (1991)

